Innovative Systems Design and Engineering
ISSN 2222-1727 (Paper) ISSN 2222-2871 (Online)
Vol 3, No 6, 2012

Design and Modeling of Hysteresis Motor with High Temperature Superconducting Material in the Rotor using Finite Element Method

Joyashree Das* Dr. Rup Narayan Ray
Department of Electrical Engineering, NIT, Agartala, West Tripura-799055, India
*E-mail of the corresponding author: joyashree_007@rediffmail.com

Abstract

In this paper, a 2-pole, 50 Hz high temperature superconducting hysteresis motor with simplest construction has been numerically simulated using finite element method for its performance calculation. In this high temperature superconducting hysteresis motor, conventional stator is used and the rotor is made up of high temperature superconducting material which has the ability to trap the magnetic field as high as possible and also carries greater current densities at higher magnetic fields. Since huge investments and time are required for the practical experiments for this work, numerical simulation are preferred. The performance parameters are compared with that of the conventional hysteresis motor in which ferro-magnetic material is used as a rotor. All of these calculations are done using MATLAB based program developed in-house and PDE based module of COMSOL Multiphysics software with proper Dirichlet and Neumann boundary conditions. The simulation result shows a good agreement with the experimental results.

Keywords: High temperature superconductor (HTS), Yttrium Barium Copper Oxide (YBCO), Finite element method (FEM), Partial differential equation (PDE), COMSOL Multiphysics.

1. Introduction

Hysteresis motor is one type of synchronous motor with uniform air gap and there is no dc excitation in the rotor because of the magnetic material used in the rotor. It utilizes the principle of hysteresis to produce mechanical torque in the rotor by virtue of hysteresis and eddy currents. The torque of a motor is proportional to the area of hysteresis loop. The rotor of hysteresis motor has no winding, no teeth thus it has quite operation. It has not only noiseless operation but also simple construction with conventional stator winding, high self-starting torque during the run-up and synchronization period [1]. These advantages make the hysteresis motor especially suitable for wide range of industrial applications. In spite of these advantages, the conventional hysteresis motor still suffers from some limitations. Thus the optimal performance study of the motor must be required. Different techniques are available to improve performance of the machine. Changing magnetic property of the rotor using different types of rotor materials is one of the techniques to improve performance of the machine. Several international research groups have explored the possibility of rotor made up of HTS materials in the construction of hysteresis machines using bulk yttrium-barium-copper-oxide (YBCO) elements [2], as superconducting materials possess higher flux density consequently current density gets increased and the developed power also gets increased. Some exclusive superiority of superconducting synchronous machines over its conventional machines have better torque to volume ratio [1], reduced size and losses for the same power [3],[4].

In this paper, 2D modeling of hysteresis motor using high temperature superconducting elements in the rotor is presented. Then the various performance parameters are numerically calculated using finite element method and these measured parameters are compared with experimental results of conventional hysteresis motor. Finally, conclusions are drawn.

2. Modeling of Hysteresis Motor

2.1 Conventional Hysteresis Motor

The main parts of hysteresis motor are stator and rotor. The stator consists of copper winding which are used to create the magnetic rotating field and that drags the rotor. The rotor is made up of hard iron ring with a high degree of

magnetic hysteresis. In this case motor shaft is made up of paramagnetic material [4]. The layout of hysteresis motor is shown in Figure (1).

2.2 Proposed High Temperature Superconducting Hysteresis Motor

Superconducting hysteresis motor is almost identical with conventional hysteresis motor but its rotor is constructed from HTS materials (YBCO). In this motor, the armature winding is built in the stator slots and consists of conventional copper conductors and stator core is made of iron. However, the rotor core is constructed with paramagnetic materials, aluminum is used as a paramagnetic material, they provide the mechanical support to the HTS elements [2] and the shaft consists of paramagnetic material such as steel. The cross-sectional view of HTS hysteresis motor is shown in Figure (2). Due to the brittle nature of YBCO materials, a single superconducting cylinder cannot be constructed. So the segments are assembled with non-magnetic materials [2], [4] Figure (3). For large shielding, more segments are advantageous [5]. If the numbers of the circular sectors are increased, the flux distribution inside the HTS rotor is also increased because of the presence of paramagnetic materials between them. But the numbers of circular sectors are limited otherwise flux leakage increases and thus the developed torque of the hysteresis motor will decrease Table (1) with increase of the number of sectors [2]. The maximum developed torque is obtained when Di=0.78D0 [5]. Where, Di and Do are the inner and outer diameter of the rotor.

3. Problem Formulation

A variable transport current is applied in the non-HTS stator of a high temperature superconducting hysteresis motor and the rotating magnetic field is produced in the air-gap. A trapped field produced in the HTS rotor due to high current carrying property. Then the various parameters of a HTS hysteresis motor are calculated using finite element method. The simulations are done using MATLAB and finite element method based COMSOL Multiphysics software.

3.1 Formulation of Electromagnetic Problem

It is known that E-H formulation is the most useful expression of an electromagnetic field [6]. These vectors measure the ability of a magnetic field to perform work on a current carrying loop. Therefore, the basic electromagnetic equation for the HTS hysteresis motor is expressed as

$$\nabla \times E = -\frac{\partial B}{\partial t} \tag{1}$$

Where, E is electric field vector [V/m] and B is magnetic flux density [T].

Therefore,

$$\nabla^2 H - \mu\sigma \frac{\partial H}{\partial t} = 0 \tag{2}$$

Here, H is magnetic field vector, $H=\begin{bmatrix} Hx \\ Hy \end{bmatrix}$

The current density (J) is obtained using the following equation

$$J= \nabla \times H \tag{3}$$

Then the electric field E is calculated using the E-j power law

$$E = Ec\left(\frac{\vec{J}}{J_C}\right)^n \tag{4}$$

Where n denotes power index, Jc is critical current density at the critical electric field (Ec).

4. Simulation and Results

The high temperature superconducting hysteresis motors are numerically simulated using finite element method based software COMSOL Multiphysics. The specifications of the high temperature superconducting material used in the rotor of the HTS hysteresis motor is shown in Table (2) and also the dimensions of the conventional and HTS hysteresis motor is shown in Table (3).

To discretize the HTS hysteresis motor into finite elements, mesh statistics are applied. From this mesh statistics Table (4), various parameters are known. Figure (4) shows the mesh of a HTS hysteresis motor.

The solution time is changed due to change in the values of various parameters but the number of elements and number of degrees of freedom will remain same unless the geometry is changed. Dirichlet condition is applied in the outer boundary and shaft and Neumann condition is applied in other boundaries.

4.1 Magnetic Flux Distribution in HTS Hysteresis Motor

Figure (5) shows the contour plot of magnetic vector potential in a HTS hysteresis motor. It is observed that two poles have been created. The stator current produces rotating field in the air gap between the stator and the rotor, which in turn induces currents in the superconductor and the HTS rotor is magnetized. Due to the high current leading ability (ξ=*Jt*Δ/*Js a*) of HTS rotor where *Jt* and *Js* are intra-granular and in-granular current densities and Δ and *a* are dimensions of HTS rotor and HTS grain, most of the fluxes are trapped in the HTS hysteresis rotor. This phenomenon is shown in the plots of flux density (B) in the rotor only of a HTS hysteresis motor in Figure (6) and the flux density plot in HTS hysteresis motor in Figure (7). From Figure (6) and Figure (7), it is observed that the magnetic flux concentration is more inside the HTS rotor compared to the other region.

4.2 Hysteresis Loop of HTS Hysteresis Motor

Due to application of alternating currents of different magnitudes in the stator conductors, different flux plots are obtained. Taking the values of magnetizations and the flux densities at different positions on the HTS rotor the hysteresis loops are plotted. For different stator currents, the areas of the hysteresis loops Figure (8) are changed. When the applied currents in the stator i.e. the rotating magnetic field in the air gap, are increased, more fluxes are trapped into the HTS material, as a result of this the area of the hysteresis loops are increased and thus the power density of the hysteresis motors are increased [7] as well as hunting will be reduced [8].

4.3 Effects of Applied Current on Torque of a HTS Hysteresis Motor

The torque is directly proportional to the area of the hysteresis loop and the area hysteresis loop is approximately proportional to the applied current that is calculated in last section. The torque in hysteresis motor is calculated using the relation, $T = \left(\frac{1}{2\Pi}\right) P V_r A_h$ [9],[10],

where, *P* is number of pole pairs, V_r is volume of the HTS rotor and A_h is area of the hysteresis loop in the HTS rotor. MATLAB program has been developed to draw the hysteresis curves and the corresponding torque developed in the motor. As shown in Figure (9), the torque changes almost linearly with the applied current, that is the common feature of any hysteresis motor [9]. The simulation result shows a good agreement with the experimental results [10],[11].

4.4 Current density plot in a HTS hysteresis motor

Due to the trapped field in the HTS hysteresis rotor, the current density also more in that region shown in Figure (10). When the trapped fields are gradually decreased in the inner part of the HTS rotor, the current density also gradually decreases and minimum in the inner part of the rotor. In addition, Figure (11) shows power index (n) versus current density plot in the HTS hysteresis motor. It is observed that the value of integral of current density is less compared to the critical current density (4 A/m^2). $\times 10^7$

5. Conclusion

In this paper modeling of high temperature superconducting hysteresis motor is presented and then the performance parameters are numerically calculated using finite element method and then compared with the experimental results of conventional hysteresis motor. The mechanical torque of HTS hysteresis motor is produced due to the repulsion of the magnetic poles (in this work number of rotor poles are two) induced into the HTS rotor by the rotating field of the stator winding. All the calculated results show a good agreement with the experimental results and it also shows that the bulk HTS material can trap higher value of magnetic field compared to ferro-magnetic material as a result of this area of the hysteresis loop is increased as well as output power increases and hunting will be reduced.

References

Nasiri-Gheidari, Z., Lesani, H. & Tootoonchian, F. (2006), "A New Hunting Control Method for Permanent Magnet Hysteresis Motors", *IJEEE* **2**(3 & 4),121-130.

Rodrigues, Leao, A. (2009), "Drum and Disc Type Hysteresis Machines with Superconducting Rotors", *IEEE*,55-59.

Match, L., and Morgan, J. (1986). *Electromagnetic and electromechanical machines*. Wiley & Sons.

Inacio, D., Inacio, S., Pina, J., Goncalves, A., Ventim, N. M. & Rodrigues, Leao, A. (2007), "Numerical and Experimental Comparison of Electromechanical Properties and Efficiency of HTS and Ferromagnetic Hysteresis Motors", *8th European Conference On Applied Superconductivity (EUCAS 2007)*,1-7.

Barnes, G. J., McCulloch, M. D. & Dew-Hughes, D. (2000), "Torque from Hysteresis Machines with Type-II Superconducting Segmented Rotors", *Physica C: Superconductivity* **331**(2),133-140.

Chari, M. V. K., and Silvester, P. P. (1980). *Finite elements in electrical and magnetic field problems*. John Willy and Sons.

Muta, I., Jung, H. J., Hirata, T., Nakamura, T., Hoshino, T. & Konishi, T. (2001), "Fundamental Experiments of Axial-Type BSCCO-Bulk Superconducting Motor Model", *IEEE Transactions On Applied Superconductivity* **II**(I),1964-1967.

Soroush, R. H., Rahmati, R. A., Moghbelli, H., Vahedi, A. & Niasar, Halvaeei, A. (2009), "Study on the Hunting in High Speed Hysteresis motors Due to the Rotor Hysteresis Material", *IEEE*,677-681.

Hong-Kyu, Kim, Sun-Ki, Hong & Hyun-Kyo, J. (2000), "Analysis of Hysteresis Motor using Finite Element Method and Magnetization-Dependent Model", *IEEE Transactions On Magnetics* **36**(4),685-688.

Sun-Ki, Hong, Hong-Kyu, Kim, Hyeong-Seok, Kim & Hyun-Kyo, J. (2000), "Torque calculation of Hysteresis Motor using Vector Hysteresis Model", *IEEE Transactions On Magnetics* **36**(4),1932-1935.

Lee, Hak-Yong, Hahn, Song-yop, Park, Gwan-Soo & Lee, Ki-Sik (1998), "Torque Computation of Hysteresis Motor using Finite Element Enalysis with Asymmetric Two Dimensional Magnetic Permeability Tensor", *IEEE Transactions On Magnetics* **34** (5),3032-3035.

Joyashree Das was born in Agartala, Tripura, in May 1986. She received the B.E. degree in Electrical Engineering from National Institute of Technology, Agartala, Tripura, India, in 2008 & the M.E. degree in Power Engineering from Jadavpur University, Kolkata, West Bengal, India, in 2010 respectively. She is currently a Research Scholar in the Department of Electrical Engineering, National Institute of Technology, Agartala. Her research interests are mainly design, implementation & optimization of electric machines.

Dr. Rup Narayan Ray presently working as an Associate Professor in the Department of Electrical Engineering at National Institute of Technology, Agartala. Dr. Ray received the B.E. degree in Electrical Engineering from Calcutta University, India & the M.E. degree in the same field from B. E. College, India. He obtained the Ph.D. degree from Jadavpur University, Kolkata, West Bengal, India. His areas of interest are mainly electrical machines & drives, power qualities & distributed generations.

Table 1. Analytical high field limits of torque [5]

Number of segments, N	1	2	3	4	6	8
High field torque limit/ Tmax	1	1	0.51	0.42	0.28	0.22

Table 2. Specifications of the HTS material used in the rotor.

Name of the sample	Outer radius (R_o) (mm)	Inner radius (R_i) (mm)	Thickness (R_o-R_i) (mm)	Critical current density (A/m^2)	Critical electric field (V/m)	Initial Conductivity (S/m)
YBCO	21.7	18.2	3.5	4×10^7	10^{-4}	10^{16}

Table 3. Dimensions of HTS and conventional hysteresis motor

Dimensions	Stator Outer Radius (mm)	Rotor Outer Radius (mm)	Rotor Inner Radius (mm)	Air-gap (mm)
HTS hysteresis motor	40	21.7	18.2	1
Conventional hysteresis motor	60	28	26.25	1

Table 4. Mesh statistics of HTS hysteresis motor

Mesh statistics	Solver	Number of elements	Number of degree of freedom	Number of boundary elements	Solution time (sec)	Processor
2-dimentional	Time dependent solver	17 432	34 754	1234	26.219	Intel(R) Core(TM)2Quad @2.50GHz

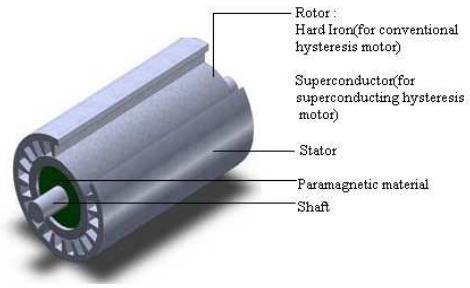

Figure 1. Hysteresis motor layout [4].

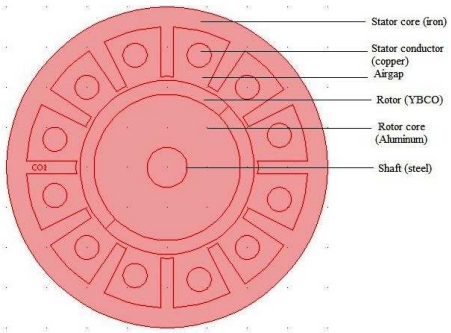

Figure 2. Cross-sectional view of HTS hysteresis motor in COMSOL MULTIPHYSICS.

Figure 3. Segmented HTS hysteresis rotor, with two or four segments [4].

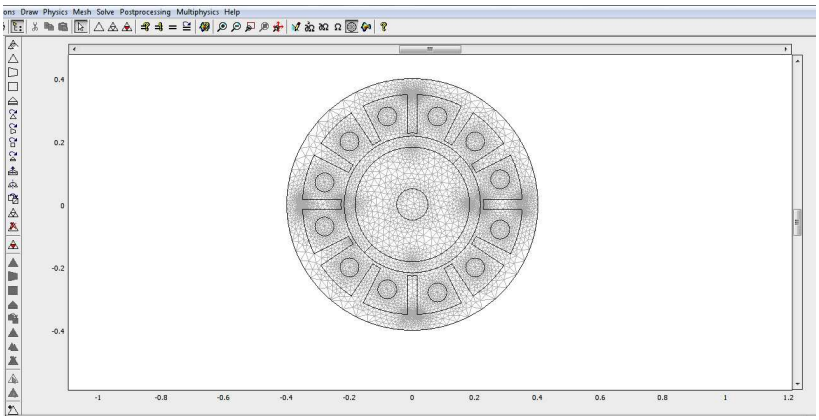

Figure 4. Mesh of HTS hysteresis motor.

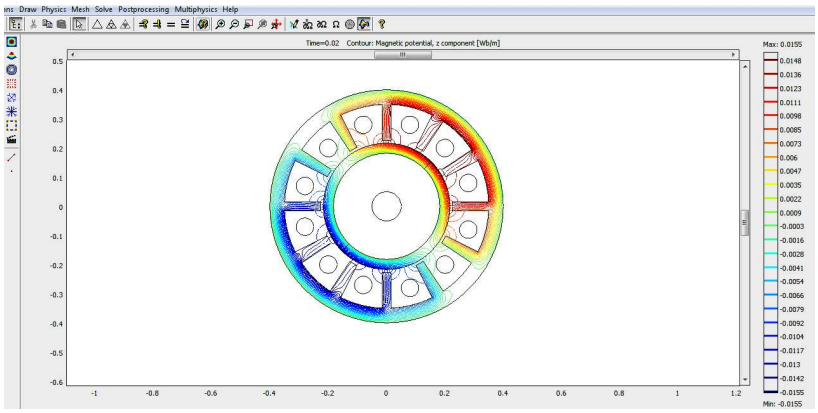

Figure 5. Magnetic potential of a HTS hysteresis motor (contour plot).

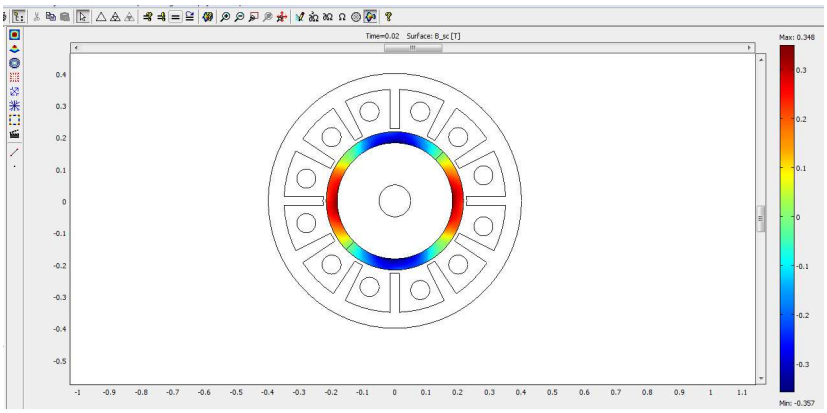

Figure 6. Magnetic flux density in the rotor only of a HTS hysteresis motor.

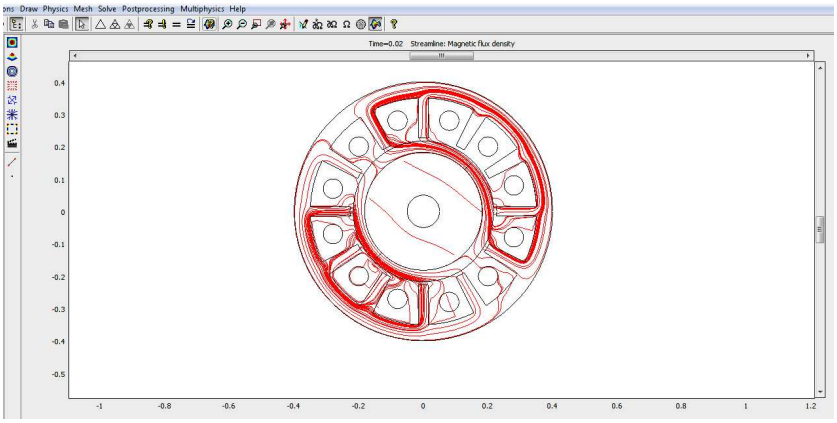

Figure 7. Magnetic flux density of a HTS hysteresis motor.

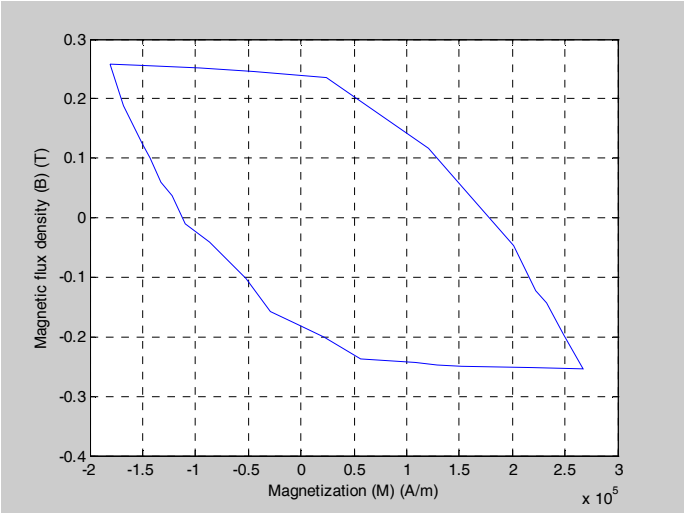

Figure 8. B-M plot of a HTS hysteresis motor at 100mA.

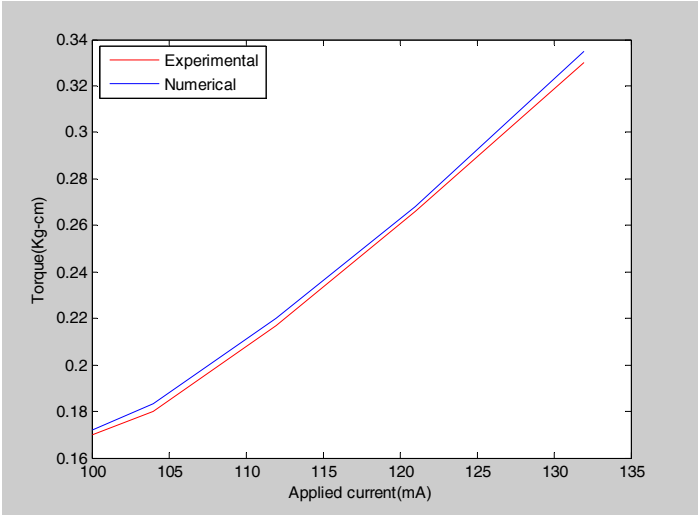

Figure 9. Simulation and experimental results of torque vs. current plot of a HTS hysteresis motor.

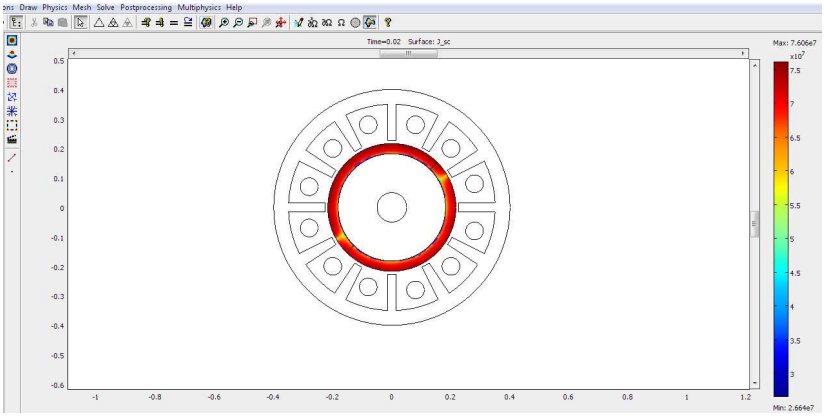

Figure 10. Current density plot of a HTS hysteresis motor.

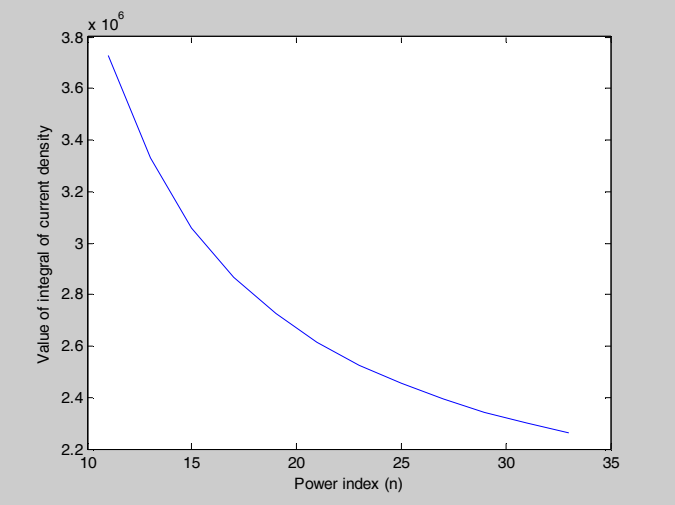

Figure 11. Power index vs. current density plot of a HTS hysteresis motor.